Structural Engineering and Mechanics, *Vol. 77, No. 3 (2021) 329-342*
DOI: https://doi.org/10.12989/sem.2021.77.3.329

Effect of rebar spacing on the behavior of concrete slabs under projectile impact

Husain Abbas[a], Nadeem A. Siddiqui[b], Tarek H. Almusallam[c], Aref A. Abadel[d], Hussein Elsanadedy[e] and Yousef A. Al-Salloum*

Chair of Research and Studies in Strengthening and Rehabilitation of Structures, Department of Civil Engineering, King Saud University, Riyadh 11421, Saudi Arabia

(Received November 25, 2019, Revised October 25, 2020, Accepted October 27, 2020)

Abstract. In this paper, the effect of different steel bar configurations on the quasi-static punching and impact response of concrete slabs was studied. A total of forty RC square slab specimens were cast in two groups of concrete strengths of 40 and 63 MPa. In each group of twenty specimens, ten specimens were reinforced at the back face (singly reinforced), and the remaining specimens were reinforced on both faces of the slab (doubly reinforced). Two rebar spacing of 25 and 100 mm, with constant reinforcement ratio and effective depth, were used in both singly and doubly reinforced slab specimens. The specimens were tested against the normal impact of cylindrical projectiles of hemispherical nose shape. Slabs were also quasi-statically tested in punching using the same projectile, which was employed for the impact testing. The experimental response illustrates that 25 mm spaced rebars are effective in (i) decreasing the local damage and overall penetration depth, (ii) increasing the absorption of impact energy, and (iii) enhancing the ballistic limit of RC slabs. The ballistic limit was predicted using the quasi-static punching test results of slab specimens showing a strong correlation between the dynamic perforation energy and the energy required for quasi-static perforation of slabs.

Keywords: RC slabs; impact; rebar spacing; quasi-static; ballistic limit; projectile

1. Introduction

Reinforced concrete (RC) slabs and walls are sometimes exposed to impact loads generated as a result of the strike of missiles, projectiles, and blast debris (e.g., Abbas *et al*. 1996, Siddiqui and Abbas 2002, Siddiqui *et al*. 2006, Siddiqui *et al*. 2014a,b, Sohn *et al*. 2014, Wu *et al*. 2015, Thai and Kim 2015, Mazek and Wahab 2015, Öncü *et al*. 2015, Tamayo and Awruch 2016, Peng *et al*. 2016, Verma *et al*. 2016, Rajput and Iqbal 2017, Wang *et al*. 2017). The resistance of RC slabs and walls against impact loads can be enhanced by various techniques. Use of closely spaced small diameter rebars (i.e., welded wire mesh) is one of the possible ways for improving the impact resistance of the slabs.

Zineddin and Krauthammer (2007) studied the dynamic response of structural concrete slabs under impact loading for improving the protective design of RC structures. The influence of various types of slab reinforcements and the impact loads on the dynamic behavior of RC slabs were investigated by testing 90×1524×3353 mm slabs reinforced with three types of reinforcements. The three reinforcement options included, two welded wire meshes of wire diameter 5 mm located under 25 mm of concrete cover; one #3 steel bar mesh placed at the mid-thickness level of the slab, and; finally two #3 steel bar meshes located under 25 mm of concrete cover on both faces of the slab. The impact experiments were conducted with an advanced impact hammer device, dropped from three different pre-determined heights of 152, 305 and 610 mm on RC slabs. The results from this experimental program showed that the slab behavior depends on the quantity of steel reinforcement and the drop height.

Abdel-Kader and Fouda (2014) studied the effect of the steel ratio and reinforcement type on the behavior of RC slabs against impact loading. They considered steel lining and embedded steel mesh on different faces of the slabs in their study. They observed that the crater sizes on the back and front faces depend on the location of the rebar mesh. They also noticed that the steel lining improves the penetration resistance substantially. Li *et al*. (2017) presented field blast tests results on RC slabs under close-in detonations. They investigated the performances of hybrid steel wire mesh-micro steel fiber reinforcement through the laboratory static tests and field blast tests. In addition, a numerical study based on Multi-Material Alternate-Lagrangian-Eulerian algorithm was performed to further

*Corresponding author, Professor
E-mail: ysalloum@ksu.edu.sa
[a]Ph.D., Professor
E-mail: habbas@ksu.edu.sa
[b]Ph.D., Professor
E-mail: nadeem@ksu.edu.sa
[c]Ph.D., Professor
E-mail: musallam@ksu.edu.sa
[d]Ph.D., Assistant Professor
E-mail: aabadel@ksu.edu.sa
[e]Ph.D., Associate Professor
E-mail: helsanadedy@ksu.edu.sa

ISSN: 1225-4568 (Print), 1598-6217 (Online)

investigate the field tests' phenomenon.

Almusallam *et al*. (2013) experimentally studied the effectiveness of hybrid fibers (steel plus plastic fibers) in enhancing the impact resistance of RC slabs. They tested 54 slab specimens of size 600×600×90 mm under the impact of steel projectiles of Bi-conic nose shape. Half of the specimens were cast using normal strength concrete whereas remaining half were made using high strength concrete. Slabs were reinforced on the face opposite to the striking face by 8 mm rebars at 100 mm c/c in both directions. They observed that the hybrid fibers are very effective in reducing the crater size, penetration depth, number of cracks and ejected mass of concrete. They also proposed analytical expressions for estimating penetration depth, ballistic limit and ejected mass of concrete from the front and rear faces of the slabs. The predictions matched well with the experimental observations. This study (Almusallam *et al*. 2013) was further extended in Almusallam *et al*. (2015) by adding 27 new hybrid-fiber reinforced slab specimens in the database. The new specimens had the same distribution of rebars (i.e., ϕ8@100 mm c/c) as before but some new combinations and proportions of steel and synthetic fibers were considered. The target compressive strength of the specimens was 60 MPa, and they were tested against the impact of hemispherical steel projectiles. This study highlights the importance of geometrical properties of hybrid fibers in improving the impact resistance of the slab specimens. In this study, the earlier proposed analytical equations for estimating ballistic limit and penetration depth were generalized to incorporate the influence of hybrid fibers made-up of any number of fibers. The predictions of the generalized equations were compared with a larger data set containing data of this study, and the data available in the literature including the previous study (Almusallam *et al*. 2013). The predictions agree well with the experimental data. Dancygier (1997) studied the effect of the reinforcement ratio on the impact resistance of RC structural elements. He also modified the existing perforation equation in order to include the effect of reinforcement ratio. The theoretical results were compared with test results and good agreement was reported. Murali and Ramprasad (2018) studied the impact behavior of layered fiber reinforced concrete (FRC) slabs. The slabs were cast in two groups. The slabs of the first group were prepared using three layers of FRC having varying percentages of different types of steel fibers. In the second group, the slabs were cast in single layer of FRC having only one type of steel fibers. The slabs were tested under repeated drop weight impact till failure. The test results showed that the number of impacts for layered FRC slabs were significantly higher than the single layer FRC slabs.

Xu *et al*. (2019) studied experimentally and predicted analytically the failure mechanism of thick RC slabs subjected to high-velocity projectile impact. They predicted and compared the rear face damage area, impact energy, and residual velocity with the experimentally observed values. They theoretically also studied the effect of reinforcement ratio on the perforation parameters and observed that the effect of the reinforcement ratio was small on these parameters. Goswami *et al*. (2019) proposed a simplified analytical procedure for predicting the punching shear failure of RC slabs under low velocity (less than 10 m/s) impact loads. They compared their prediction with their numerical simulations and experimental results available in the literature.

The review of the available literature indicates that there are limited studies on the influence of rebar spacing on the impact response of RC slabs. Although a few researches are available on the effect of varying percentage of reinforcement on impact response of RC, effect of rebar spacing for a same percentage of reinforcement and effective depth has not been studied. In the present paper, the influence of the rebar spacing was studied on impact response of singly and doubly reinforced slabs of two different concrete grades for the same percentage of rebars and effective depth. The specimens were tested against the normal impact of cylindrical projectiles of hemispherical nose shape. Slabs were also quasi-statically tested in punching using the same projectile which was employed for the impact testing. The effect of rebar spacing was studied on (i) the overall penetration depth and local damage, (ii) energy absorption capacity and (iii) ballistic limit of RC slabs. The ballistic limit velocity was predicted using the test results of the quasi-static punching of RC slabs for establishing a correlation between the dynamic perforation energy and the energy required for quasi-static perforation of slabs.

2. Experimental program

In the current experimental program, a total of forty square RC slab specimens of 600 mm size and 90 mm thickness were prepared in two groups of concrete strengths of 40 and 63 MPa. In each group of twenty specimens, ten specimens were reinforced only at the rear face of the slab (i.e., singly reinforced), whereas the remaining ten specimens were doubly reinforced (i.e., reinforcement was provided on the front as well as on the back face of the slabs). The slab specimens were tested against the normal impact of steel projectiles of 40 mm diameter having hemispherical nose shape. Slabs were also tested under the quasi-static punching load applied through the same 40 mm diameter cylindrical steel projectile which was employed for the impact testing.

To study the effect of rebar spacing, at constant reinforcement percentage and effective depth, two rebar spacings, 100 mm or 25 mm, were used. For 100 mm rebar spacing, slab specimens were reinforced with 8 mm diameter bars provided at 100 mm c/c spacing (0.7% steel), whereas for reduced rebar spacing of 25 mm, specimens were reinforced with two layers of welded wire mesh (WWM) of ϕ4@50 mm c/c, equivalent to ϕ4@25 mm c/c giving the same reinforcement percentage of 0.7%. It is worth mentioning that the reinforcement ratio adopted in the study falls within the practical range of reinforcement generally provided in RC walls. The two layers of WWM were having offset of 25 mm (i.e., half mesh spacing) in the two transverse directions, which resulted in the spacing

between the bars as 25 mm in both directions (Fig. 1). The use of two layers of WWM meshes helped in maintaining the effective depth same as that of control.

It may be noted that if the single layer of WWM mesh of ϕ4@25 mm c/c was used it would have resulted in higher effective depth. This helped in maintaining both the effective depth and the steel ratio approximately the same in the two reinforcement schemes. Fig. 1 illustrates the details of the two reinforcement schemes. It is worth noting that the selection of the rebar diameter and rebar spacing was based on achieving almost the same percentage of steel for the two spacings of rebars. The WWM of ϕ4@50 mm was commercially available, and ϕ8@100 mm was selected for giving the same percentage of reinforcement as two layers of WWM mesh (i.e., ϕ4@25 mm).

Based on the two spacing of rebars, two grades of concrete, and two faces of reinforcement, the slabs were divided into eight subgroups namely M1-100-S, M1-100-D, M1-25-S, M1-25-D; M2-100-S, M2-100-D, M2-25-S, and M2-25-D. In this nomenclature, M1 and M2 represent the compressive strength of concrete in MPa (40 or 63 MPa); 100 and 25 represent the spacing of rebars in mm; S and D denote whether the slab is singly reinforced or doubly reinforced. In the singly reinforced slab, rebars were provided only on the rear face of slab. Five slab specimens were prepared in each subgroup, which makes a total of forty slabs. In each subgroup, one slab was used for assessing the quasi-static punching strength and remaining four slab specimens were tested against projectile impact. Table 1 illustrates the test matrix.

2.1 Materials and their properties

2.1.1 Concrete

Two mixes of concrete, M1 and M2, were used in the preparation of specimens. The compressive strengths of mix M1 and M2 were 40 and 63 MPa respectively. The two mixes represent normal and high strength concretes, respectively (ACI 318-14). The concretes of desired strength were supplied by a local ready-mix plant. Type I Portland cement was used in the preparation of concrete. The aggregates were a mixture of fine and coarse aggregates. Fine aggregates were the mixture of silica and white sands; coarse aggregates, on the other hand, were crushed limestone of maximum size 10 mm.

2.1.2 Reinforcing steel

The 8 mm rebars and 4 mm bars were tested in accordance with ASTM A370 (2017). Three specimens of rebars were tested using Universal tensile testing machine with hydraulic grips. The average yield and tensile strengths of three specimens of 8 mm rebars were 510 and 538 MPa respectively. These values for 4 mm rebars were 317 and 349 MPa respectively.

2.1.3 Projectiles

A hemispherical nosed steel projectile of 40 mm diameter was employed in the present study. The projectile mass was 0.8 kg. The projectile employed for impact testing was also used as a penetrator for quasi-static testing of slab panels.

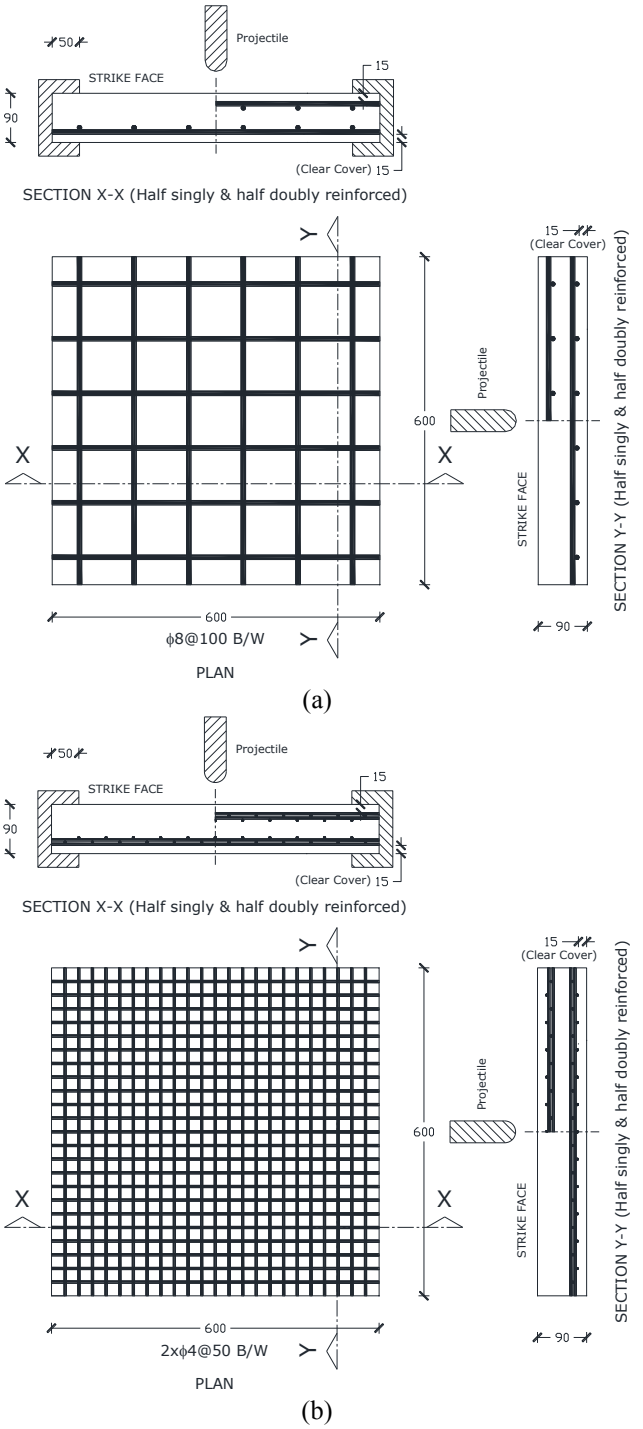

Fig. 1 Reinforcement details of test specimens: (a) slab reinforced with 100 mm spaced rebars; (b) slab reinforced with 25 mm spaced rebars (Note: All dimensions are in mm)

2.1.4 Specimen preparation

The test specimens were cast with the help of wooden molds. The steel skeleton was placed in these wooden molds and the concrete of desired strength was poured into the molds. The concrete was put in a single layer and then compacted using a pin vibrator. After the casting, the top surface of the slab was screeded and then covered with moist burlap and polythene sheets. The specimens were

Table 1 Test matrix

Specimen ID	Concrete mix	Rebar spacing (mm)	Singly (S)/ Doubly (D) reinforced	No. of specimens	Type of test*
M1-100-S-1	M1	100	S	1	QP
M1-100-S-i	M1	100	S	4 (i = 2 to 5)	Impact
M1-25-S-1	M1	25	S	1	QP
M1-25-S-i	M1	25	S	4 (i = 2 to 5)	Impact
M2-100-S-1	M2	100	S	1	QP
M2-100-S-i	M2	100	S	4 (i = 2 to 5)	Impact
M2-25-S-1	M2	25	S	1	QP
M2-25-S-i	M2	25	S	4 (i = 2 to 5)	Impact
M1-100-D-1	M1	100	D	1	QP
M1-100-D-i	M1	100	D	4 (i = 2 to 5)	Impact
M1-25-D-1	M1	25	D	1	QP
M1-25-D-i	M1	25	D	4 (i = 2 to 5)	Impact
M2-100-D-1	M2	100	D	1	QP
M2-100-D-i	M2	100	D	4 (i = 2 to 5)	Impact
M2-25-D-1	M2	25	D	1	QP
M2-25-D-i	M2	25	D	4 (i = 2 to 5)	Impact
			Total =	40	

* QP: Quasi-static punching

then subject to intermittent spraying of water on every day for two weeks. The standard concrete cylinders of size 150×300 mm were also cast for each grade of concrete. These concrete cylinders were put for curing in water tank for four weeks (28 days) and then tested as per ASTM C39 (2020). The average compressive strength of the two mixes M1 and M2 were 40 and 63 MPa respectively.

It is worth mentioning that the present study is pertaining to thin RC structural elements such as RC walls and slabs whose thicknesses vary in the range of 150 mm to 200 mm. The thickness of the slab used in the present study is roughly ½ of the average thickness of RC slabs or walls. As reported by Dönmez and Bažant (2017), the size effect for punching of RC slabs becomes almost insignificant when the thickness of the member is less than 500 mm. Thus, the thickness of the slab adopted in the present study is expected to be free from the size effect. Similar scaled specimens have also been tested for punching of RC slabs by Al-Gasham *et al*. (2019).

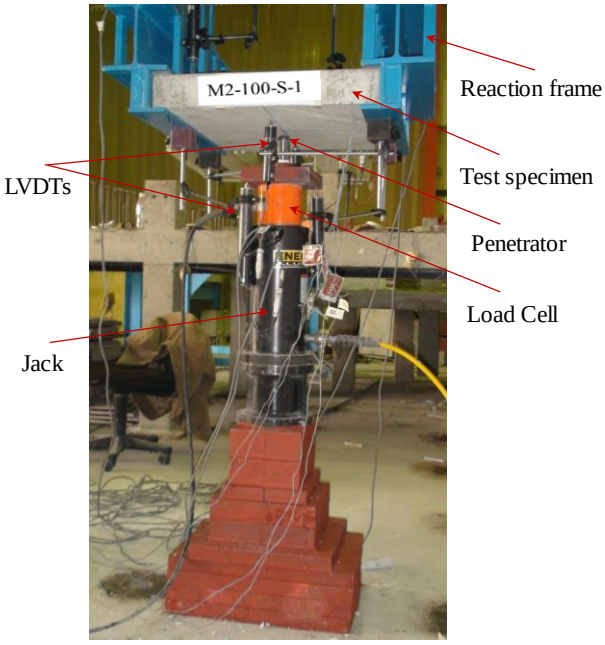

Fig. 2 Test setup for quasi-static punching test of RC slabs using projectile as a penetrator

3. Quasi-Static punching test of RC slabs

In the first phase of the present study, slabs were tested against a quasi-static punching load. The punching load was applied through a 40 mm diameter steel cylindrical penetrator having a spherical nose. The same penetrator (as projectile) was later used for the impact test. The slabs were clamped on the two opposite edges (as employed in the projectile impact tests) and were subjected to punching load. The load was applied at the center in such a manner that no rebar in M1-100 and M2-100 slabs comes in along the line of action of the force. Thus, the location of the applied load for these slabs had minimum punching resistance. However, for M1-25 and M2-25 slabs, due to closer spacing, the projectile was intercepted by the rebars. The quasi-static load was applied on the specimens through spherical nosed projectile at the rate of 18 kN/min until failure (Abbas *et al*. 2015). A data logger was used to measure the incremental load and corresponding displacements (Fig. 2).

3.1 Effect of rebar spacing on slab damage

Fig. 3 illustrates the failure pattern observed during Quasi-static testing of singly and doubly reinforced slabs. The slab specimens prepared using mixes M1 and M2 illustrate that the concrete slabs of higher compressive strength experienced lesser damage than the slab having lower strength. Fig. 3 also illustrates that all the specimens

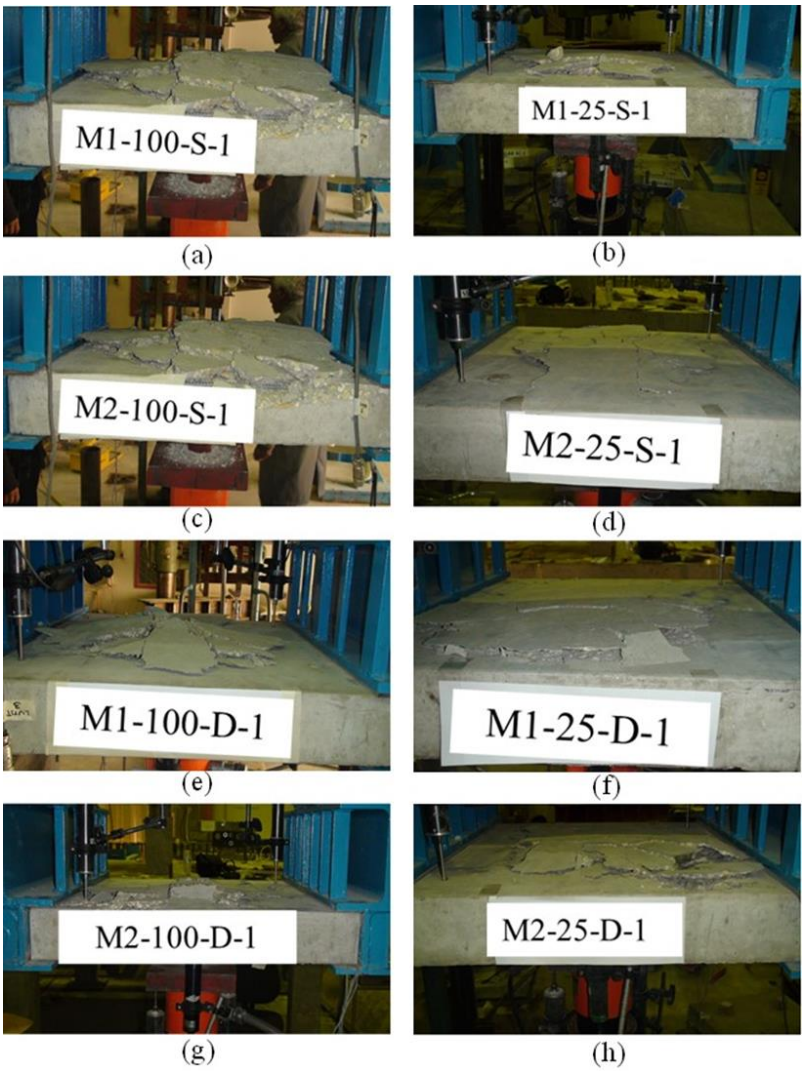

Fig. 3 Punching shear failure of RC slabs: (a) M1-100-S-1; (b) M1-25-S-1; (c) M2-100-S-1; (d) M2-25-S-1; (e) M1-100-D-1; (f) M1-25-D-1; (g) M2-100-D-1; (h) M2-25-D-1

having 25 mm spaced rebars had lesser local damage than specimens with 100 mm spacing of rebars. This is expected because there is a lesser resistance to punching when bars are far apart. Similarly, when the reinforcement is provided on both the faces (i.e. doubly reinforced slabs), the damage of slabs was observed substantially less than when the rebars are provided only on the back face. This is again because of the increase of punching resistance of slab due to the presence of front face reinforcement.

3.2 Effect of rebar spacing on load-displacement behavior

Figs. 4(a) and 4(b) depict the load-displacement response of the RC slab specimens of two mixes of concrete M1 and M2, respectively. However, due to the membrane action in 25 mm rebar spaced slabs, the response of the two slabs differs after the occurrence of the cracks. The membrane action primarily occurred in 25 mm rebar spaced slabs because the penetrator pushed the rebar cage as the rebars directly intercepted it, and it was not possible for the penetrator to punch the slab without pushing the rebar cage. It is interesting to note that there are two peak loads for 25 mm rebar spaced slabs. However, the second peak in 100 mm rebar spaced slabs is not sharp and distinct for lower grade of concrete (M1), instead it appeared as a flat plateau because the penetrator (diameter, 40 mm) punches the slab without significantly affecting the rebars in the vicinity. Nevertheless, for high strength concrete with 100 mm spaced rebars, there is significant load transfer to the rebars and due to which the second peak appeared in the load-deformation curve. The dowel action of the rear face rebars was the prime cause of the appearance of the second peak load. As the spacing between the rebars was closer in 25 mm spaced rebar slabs, the dowel action was more dominant in these slabs leading to the development of a distinct second peak. This finding is different from the earlier observations (Oh and Sim 2004, Reinhardt and Walraven 1982, Rochdi *et al.* 2006) as the earlier researchers added the dowel force of rebars in their estimation of the punching shear resistance of RC slabs (i.e., the first peak load). It is worth mentioning that the load-displacement diagrams are drawn up to 40 mm displacements as the resistance offered by the slabs beyond

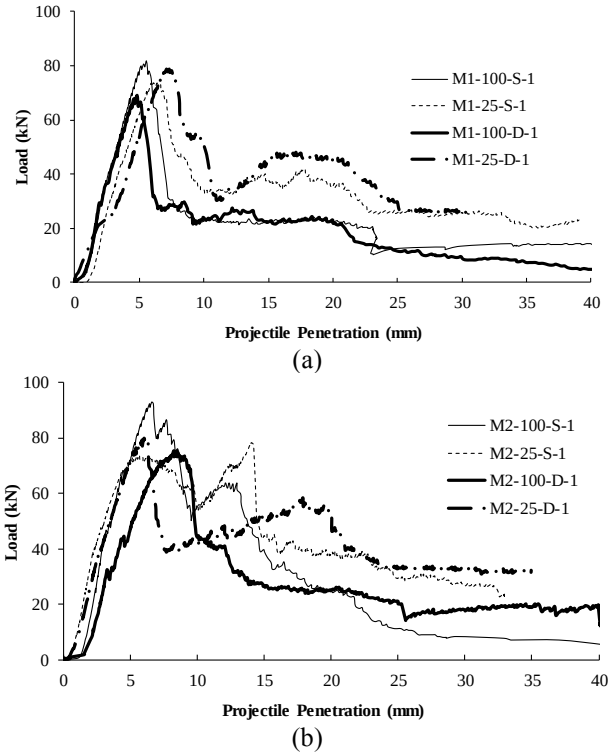

Fig. 4 Load-penetration curves for quasi-static punching in 100 mm and 25 mm spaced rebar RC slabs of: (a) Mix M1; (b) Mix M2

40 mm was insignificant for all the tested specimens.

For the 25 mm rebar spaced singly reinforced slabs, there is a little decrease in the first peak (10% for concrete mix M1 and 20% for concrete mix M2). However, the second peak is substantially higher (about 75% for concrete mix M1 and 23% for concrete mix M2) than the 100 mm rebar spaced slab. Whereas for doubly reinforced slabs of 25 mm spaced rebars, first peak load is slightly higher (about 14% for mix M1 and 7% for mix M2) than the 100 mm rebar spaced slabs but the second peak load is considerably more than 100 mm rebar spaced slabs (about 69% for mix M1 and 118% for mix M2). This higher increase can be attributed to the dowel action provided by the top and bottom layers of reinforcement in doubly reinforced slabs.

3.3 Effect of rebar spacing on energy absorption

Figs. 5(a) and 5(b) show the amount of energy absorbed during quasi-static punching of RC slabs of concrete mixes M1 and M2 respectively. The energy absorbed was estimated up to a projectile penetration of 30 mm (i.e., 1/3 of the slab thickness) because the energy absorption beyond this limit was almost insignificant in all the tested specimens. For both 25 mm rebar spaced singly and doubly reinforced slabs, there is a substantial increase in the energy absorption of RC slabs during quasi-static punching. For singly reinforced slabs, the increase in energy absorption varies from 30% to 40%, whereas for doubly reinforced slabs, it ranges from 43% to 65%. In 25 mm rebar spaced slabs, the closer spacing of rebars resists the projectile penetration of the punching cone due to membrane action. This leads to the formation of the second peak resulting in the increase in the energy absorption. The increase in the energy absorption for the slabs of 25 mm spaced rebars is also due to the enhanced crushing and cracking resistance of concrete (due to reduced rebars spacing).

4. Impact testing of slabs

The impact testing facility developed at King Saud University was used for testing of RC slabs, clamped on the two opposite edges, against the projectile impact. The projectiles were fired at the desired velocities using the impact penetration tester (Fig. 6). The wider spaced rebar slabs (M1-100 and M2-100) were positioned so as avoid the strike of the projectile on the rebars. However, in M1-25 and M2-25 slabs, the projectiles were intercepted by the rebars due to closer spacing of the rebars in these slabs. The projectile employed for impact tests was the same as the penetrator used in the quasi-static tests.

The slab damage was assessed in terms of the front and back crater sizes measured as the diameter of the equivalent circle, D_{eq}, using the procedure proposed by Dancygier *et al.* (2007). The penetration depth on the front face was also recorded. According to Dancygier *et al.* (2007), slab damage can be assessed with the help of six levels, which are:

Through-thickness cracking	Level 1: Damage on the rear face is very small and not visible by naked eyes or having a few hairline cracks.
	Level 2: Cracks on the back face are clearly visible with no scabbing.
	Level 3: Cracks are extensive, and crater develops on the rear face along with the formation of the shear plug.
Scabbing	Level 4: Substantial damage on the back face, an indication of spalling, scabbing, and/or the formation of a shear plug with no perforation.
Perforation	Level 5: Specimen was perforated, but projectile did not exit the slab. In 25 mm spaced rebar slabs, rebars were cut.
	Level 6: The slab was perforated, and projectile exited with some residual velocity. In 25 mm spaced rebar slabs, rebars were cut.

The above six levels are categorized under three subheads as indicated above. Table 2 illustrates the damage levels according to the above scales. The measured depth of penetration and the crater sizes observed in 100 mm and 25 mm rebar spaced slab specimens are also provided in this table.

4.1 Effect of rebar spacing on impact response of RC slabs

4.1.1 Slab damage under the same strike velocity

For studying the influence of rebar spacing on slab

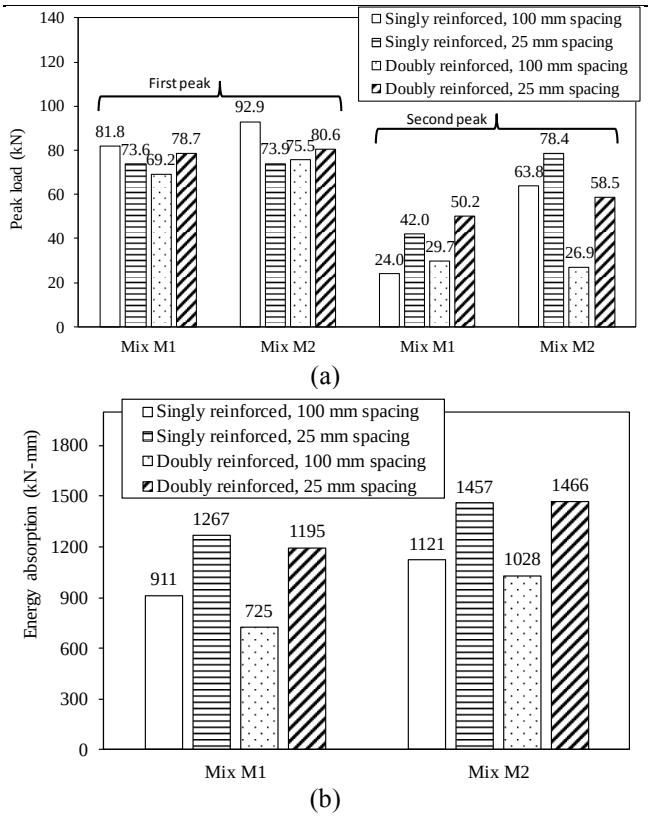

Fig. 5 Comparison of quasi-static test results of 100 mm and 25 mm spaced rebar RC slabs for: (a) Peak loads; (b) Energy absorbed

damage, sets of specimens were grouped by selecting the two specimens one from 100 mm and another from 25 mm rebar spacing having same strike velocity. Four sets meeting the above criteria are as follows:

Set 1 (Singly reinforced): M1-100-S-2 and M1-25-S-2 (Strike velocity ≅ 108 m/s)

Set 2 (Singly reinforced): M1-100-S-3 and M1-25-S-3 (Strike velocity ≅ 125 m/s)

Set 3 (Singly reinforced): M2-100-S-4 and M2-25-S-2 (Strike velocity ≅ 135 m/s)

Set 4 (Doubly reinforced): M2-100-D-5 and M2-25-D-2 (Strike velocity ≅ 147 m/s)

Thus, from singly reinforced slabs, there were two sets of slabs of concrete mix M1 and one set of the slab of mix M2, whereas there was one set of doubly reinforced slabs of mix M2.

The damage observed in the singly and doubly reinforced slabs of a set are compared in Tables 3(a) and 3(b) respectively. For the slabs having 25 mm spaced rebars, the partial concrete cover remains loosely connected with the rebars but in the slabs having widely spaced rebars, concrete cover gets dislodged due to a wider spacing of rebars. The table illustrates that the damage caused on the front face by the projectile strike on the two types of slabs having closely and widely spaced rebars is almost the same, but their back-face damage is different. The damage on the rear face in singly reinforced slabs of 100 mm spaced rebars is either almost same or extends to a smaller area than the singly reinforced slabs of 25 mm spaced rebars. However,

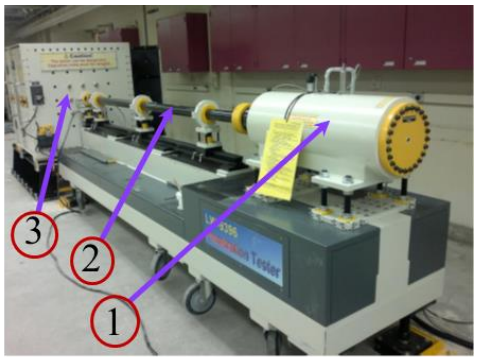

Fig. 6 Impact penetration tester (1-Gas chamber; 2-Guide barrel; and 3-Target frame)

the more concrete mass is detached in the slabs of 100 mm spaced rebars than 25 mm spaced rebars, which is due to the detachment of cover because of the bending of rebars. The damage in the slabs of 25 mm spaced rebars of concrete grade M1 increases with the increase in strike velocity from 108 to 135 m/s.

4.1.2 Slab damage at the ballistic limit

The observed damage pattern on the front and back faces of the slabs at the perforation velocity are shown in Tables 4(a) and 4(b). When the projectile impacts M1-100 and M2-100 slabs at the perforation velocity, the projectile forms a clear hole in concrete without causing significant deformations in the rebars. However, the perforation of M1-25 and M2-25 slabs at perforation velocity is after the rupture of two rebars. The projectile strike on the rebars causes deformation of steel bars which consequently results in back face cracking on the wider area. The rear face damage on 100 mm spaced rebar slabs was limited because the projectile was not intercepted by the rebars during the process of perforation.

4.1.3 Crater size and ejected weight

Table 2 illustrates the variation of crater diameters in the front and the rear faces of different slab specimens. The damage pattern observed in the slabs illustrates that the sizes of the crater were, in general, smaller in doubly reinforced slabs than singly reinforced slabs.

The variation of front and back face equivalent crater diameters and the ejected weights for the same four sets of specimens identified in Sec. 4.1.1 are illustrated in Fig. 7. In each set, there are two slabs – one is having 100 mm spaced rebars and the other is having 25 mm spaced rebars but the strike velocity for the two slabs is the same. For singly reinforced slabs, there is a clear trend of reduction in ejected weights with the reduction in rebar spacing. However, the crater diameters, both at front and back faces, are either almost same or slightly bigger in slabs having 25 mm spaced rebars. Despite having larger crater diameter, the ejected weight in 25 mm spaced rebar slabs is less due to its smaller back face crater depth as the damage in these slabs is in the concrete cover only. The decrease in ejected weight of 25 mm spaced rebar slabs is substantially higher for concrete mix M2 compared to M1 due to the brittle nature of the high strength concrete (mix M2). It is to be

Table 2 Summary of the impact test results

Specimen name	Striking velocity (m/s)	Penetration depth* (mm)	Damage level/ type	Ejected mass and crater size (Deq)			
				Front face		Rear face	
				Ejected mass (g)	Deq (mm)	Ejected mass (g)	Deq (mm)
M1-100-S-1	Tested under quasi-static punching						
M1-100-S-2	108	27.4	3	155	117	1685	390
M1-100-S-3	125	P	4/5	178	147	2391	346
M1-100-S-4	135	P	6	184	145	1520	237
M1-100-S-5	92	20.0	2	74	100	595	269
M1-25-S-1	Tested under quasi-static punching						
M1-25-S-2	108	34.1	2	85	99	1518	392
M1-25-S-3	125	34.2	3	154	135	2468	360
M1-25-S-4	147.5	P	4	586	165	3068	345
M1-25-S-5	161.3	P	5	231	145	2171	420
M2-100-S-1	Tested under quasi-static punching						
M2-100-S-2	108	27.5	2/3	95	107	3006	364
M2-100-S-3	125	P	4	151	112	2145	291
M2-100-S-4	135	P	5	383	111	4778	447
M2-100-S-5	128.5	P	4	176	127	2448	296
M2-25-S-1	Tested under quasi-static punching						
M2-25-S-2	135	35.7	2/3	169	127	1711	385
M2-25-S-3	161.3	P	4	352	160	4000	355
M2-25-S-4	178.5	P	5	171	135	3000	320
M1-100-D-1	Tested under quasi-static punching						
M1-100-D-2	108	43.7	3	130	100	2245	320
M1-100-D-3	130	P	5	105	105	175	262
M1-100-D-5	90.9	23.9	2/3	120	120	1571	300
M1-25-D-1	Tested under quasi-static punching						
M1-25-D-3	125	30.3	2/3	100	130	2370	344
M1-25-D-4	147.5	51.4	3/4	70	130	2871	340
M1-25-D-5	169	P	5	217	145	3180	325
M2-100-D-1	Tested under quasi-static punching						
M2-100-D-2	108	23.0	2	156	134	2253	394
M2-100-D-3	125	33.0	3	171	128	3649	397
M2-100-D-4	135.1	P	5	65	105	2480	348
M2-100-D-5	147.5	P	6	287	141	1804	274
M2-25-D-1	Tested under quasi-static punching						
M2-25-D-2	147.5	39.6	3	161	136	2759	359
M2-25-D-3	178	P	4	194	140	3205	335
M2-25-D-4	185	P	5	359	170	3166	350

*P: perforation.

noted that although the quantity of steel is the same in 100 mm and 25 mm rebar spaced slabs, the deformability of 25 mm rebar spaced slabs is higher because of the closer spacing of its rebars. The smaller yield strength of rebars in these slabs, compared to 8 mm rebars used in 100 mm rebar spaced slabs, was also responsible for the enhanced deformability of 25 mm rebar spaced slabs.

However, for doubly reinforced slabs, although there is a decrease in the crater diameter of the front face and the ejected weight, the trend is just opposite for the rear face as the decrease in rebar spacing causes increase in crater diameter and hence the ejected weight. The increase in crater size for reduced rebar spacing can be justified with the help of projectile penetration mechanics, as explained in Fig. 7. When projectile strikes the slab having 100 mm spaced rebars, the concrete crushes and the penetration of projectile is resisted by the surrounding confined concrete leading to a smaller back face crater size. The surrounding concrete is able to provide the confinement because the concrete is still bonded to the undamaged front rebars.

However, for slabs reinforced with 25 mm spaced ϕ4 rebars, the projectile ruptures the rebars resulting in the bending of front rebar cage which leads to the larger back face crater.

5. Analytical predictions

UKAEA (Almusallam *et al.* 2013, Li *et al*. 2005) formula given below is one of the most popular formulas

Table 3(a) Damage caused to 100 and 25-mm rebar spaced singly reinforced slabs at same strike velocity

		100 mm rebar spaced singly reinforced slabs		25 mm rebar spaced singly reinforced slabs	
Set-1: Velocity of strike = 108 m/s	Front face		M1-100-S-2 No radial crack appeared on the face of the slab	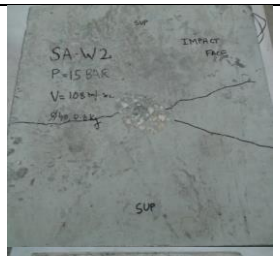	M1-25-S-2 Few radial cracks were seen originating from the ends of the crater (because projectile pushes the mesh)
	Back face		Crater size and spalling are almost the same. Rebars were bent slightly.		Crater size and spalling are almost the same. Mesh bending is more (because projectile pushes the mesh). WWM holding loose concrete.
Set-2: Velocity of strike = 125 m/s	Front face		M1-100-S-3 Few radial cracks. Diameter of hole is less than the projectile diameter.		M1-25-S-3 Few radial cracks. No hole is formed and crater size is slightly less. Concrete under projectile nose gets crushed.
	Back face		Few radial cracks. Projectile could not perforate the slab. Steel bars were bent slightly.		More radial cracks. Mesh bending is more.
Set-3: Velocity of strike = 135 m/s	Front face		M2-100-S-4 Damage was limited. Almost a complete hole was formed.	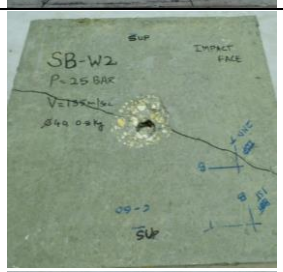	M2-25-S-2 The damage was almost the same. No hole was formed. Concrete projectile nose gets crushed.
	Back face		Projectile perforated the slab. Bars were bent substantially and substantial mass of the concrete was ejected.	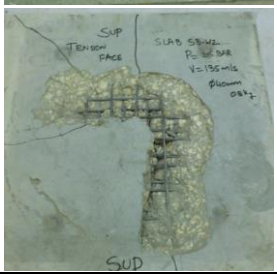	Projectile could not perforate the slab, but bent the WWM substantially. WWM held the loose concrete.

for predicting the ballistic limit for reinforced concrete targets subject to projectile impact. This formula is the updated version of the CEA-EDF formula (Li *et al*. 2005). According to this formula, ballistic limit for RC targets can be estimated as

$$V_p = V_a \quad \text{for } V_a \leq 70 \text{ m/s} \tag{1}$$

$$V_p = V_a \left[1 + \left(\frac{V_a}{500}\right)^2\right] \quad \text{for } V_a > 70 \text{ m/s} \tag{2}$$

In which,

$$V_a = 1.3\rho_c^{1/6} f_c'^{1/2} \left(\frac{pH_0^2}{\pi M}\right)^{2/3} (r + 0.3)^{1/2} \zeta \tag{3}$$

where,

$$\zeta = 1.2 - 0.6\left(\frac{c_r}{H_0}\right) \tag{4}$$

Table 3(b) Damage caused to 100 and 25 mm rebar spaced doubly reinforced slabs at same strike velocity

		100 mm rebar spaced doubly reinforced slabs		25 mm rebar spaced doubly reinforced slabs	
Set-4: Velocity of strike = 147.5 m/s	Front face		M2-100-D-5 Very few radial cracks were observed but rebars were still not visible on the impact face	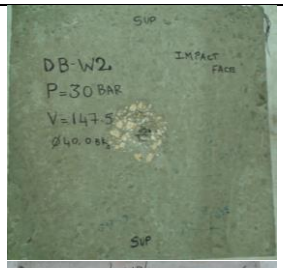	M2-25-D-2 Front face rebars visible; Rebars were bent.
	Back face	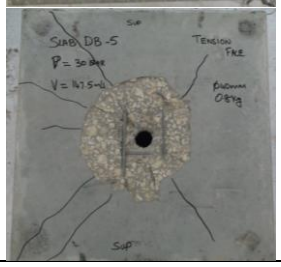	Total perforation of the slab with some radial cracks; No visible bending in steel rebars; Projectile passed through to the other side.	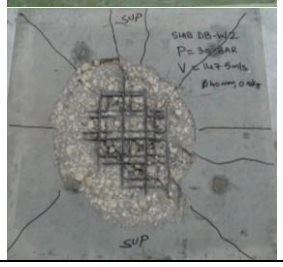	WWM rebars bent in both directions; Crater formed with radial cracks.

Table 4(a) Damage caused to 100 and 25 mm rebar spaced singly reinforced slabs at ballistic limit

		Front face damage	Back face damage	Remarks
Slabs: M1-100-S-4* & M1-25-S-5**	V_{BL} = 135.1 m/s*			Only few radial cracks were observed. Projectile passed without causing much bending in rebars.
	V_{BL} = 161.3 m/s**	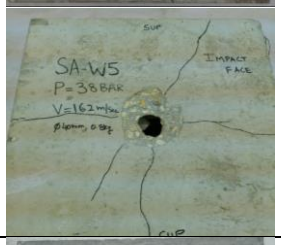	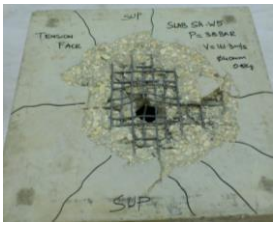	Almost same radial cracks. Front face damage was almost the same. Two bars (one in each direction) broken. Concrete spalling from back face was more. Mesh in crater zone gets detached from the concrete.
Slabs: M2-100-S-4* & M2-25-S-4**	V_{BL} = 135.0 m/s*		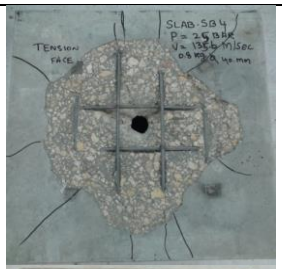	Only few radial cracks were observed. Rebars in crater zone bent and separated from the concrete in the vicinity of the hole.
	V_{BL} = 178.5 m/s**		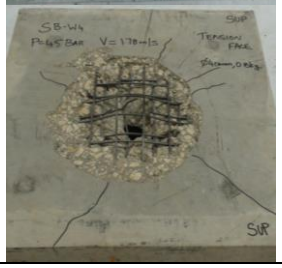	Almost same radial cracks. Front face damage was almost the same. Two bars (one in each direction) broken. Concrete spalling from back face was almost the same. Mesh in crater zone bent and detached from the concrete.

and p=perimeter of the cross-section of the projectile in m; c_r=spacing of reinforcing bars in m; r=rebar percentage; M=projectile mass in kg; H_0=RC slab thickness in m; ρ_c=concrete density in kg/m^3; f_c'=compressive strength of concrete in MPa.

when $f_c' > 37$ MPa the value of f_c' is taken as 37 MPa.

Table 4(b) Damage caused to the 100 mm spaced rebar and 25 mm spaced rebar doubly reinforced slabs at ballistic limit

	Front face damage	Back face damage	Remarks
Slabs: M1-100-D-3* & M1-25-D-5** V_{BL} = 130 m/s*			Front: Small damage area was created; Bars on impact face were not visible; Few radial cracks can be seen. Back: Rebars bent in both directions; Concrete damaged excessively.
V_{BL} = 169 m/s**		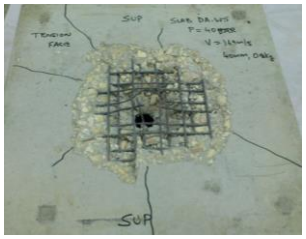	Front: WWM broken on front impact face; Very few radial cracks were noticed. Back: Both meshes were broken; Minor radial cracks were observed. Loose concrete was found between WWM meshes.
Slabs: M2-100-D-4* & M2-25-D-4** V_{BL} = 135.1 m/s*		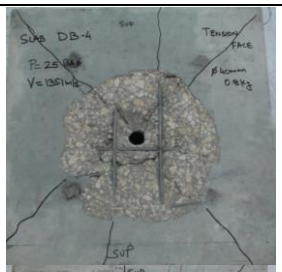	Front: Very few radial cracks were observed. Back: Rebars in tension face slightly bent in both directions. Radial cracks on tension face. Crater formed but projectile did not pass through.
V_{BL} = 185 m/s**		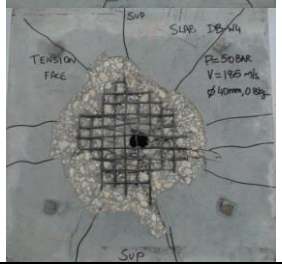	Front: WWM broken in both directions. Lots of radial cracks were observed. Back: WWM broken in both directions. Crater formed. Some loose concrete still held by steel rebars. Projectile passed through the other side.

Moreover, when $\frac{c_r}{H_0} > 0.49$, ζ is taken as 1.0, and there is no restriction on f_c'.

5.1 Prediction of the ballistic limit

As the same projectile was used in quasi-static testing of concrete slabs in punching, the energy absorbed was employed for assessing the ballistic limit. The perforation energy of slabs under projectile impact is greater than the energy absorbed in quasi-static penetration of slabs owing to the strain rate effect during impact loading. The perforation resistance of slab for a projectile of mass *M* is expressed in terms of:

$$z = \rho_c^{\frac{1}{6}} f_c'^{\frac{1}{2}} \left(\frac{pH_0^2}{\pi M}\right)^{2/3} \times (r+0.3)^{1/2} \left[1.2\text{-}0.6\left(\frac{c_r}{H_0}\right)\right] \quad (5)$$

where, *z* = perforation resistance parameter.

The above expression of perforation resistance is the same as that used in UKAEA formula of ballistic limit (Almusallam *et al.* 2013, Li *et al.* 2005). The variation of the ratio of projectile kinetic energy to the energy used in quasi-static punching is plotted against the parameter, z (Fig. 8). A line is drawn in this figure to demarcate the perforation data from non-perforation data. All the test data are following the desired trend except one data point. This data point is also not far from the line of demarcation. Thus, this line represents the perforation limit, and can be mathematically represented by the following expression:

$$\frac{E_p}{E_s} = \alpha z + \beta \quad (6)$$

where E_p is the energy required for the perforation of the slab, E_s is the energy absorbed in quasi-static punching of the slab, α and β are the model parameters, which are obtained as 0.007 and 4.6 respectively. It is worth mentioning that Eq. (6) is basically the same as the dynamic increase factor commonly used in dynamic analysis. In the present study, a concept was given through Eq. (6) for correlating quasi-static response (which is easier to perform) to impact behavior. However, in the present study, the value of E_s used in Eq. (6) was taken from the experiment. In the future, when sufficient data would be available, an equation can be developed for the estimation of E_s. Eq. (6) was employed to calculate E_p, which was then used for the estimation of the ballistic limit, as follows:

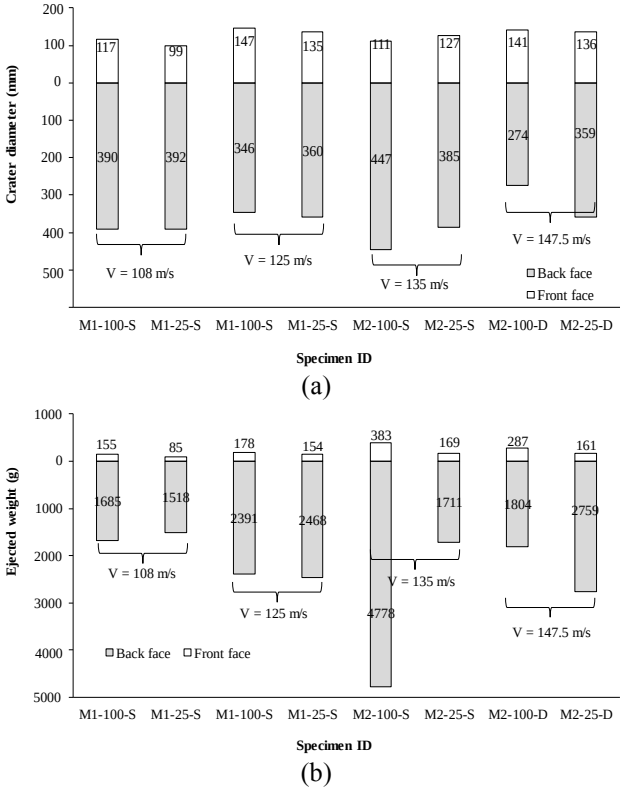

Fig. 7 Effect of rebar spacing at the same strike velocity on: (a) equivalent crater diameter on front and back faces; and (b) ejected weight from front and back faces (V = Strike velocity)

$$V_p = \sqrt{\frac{2E_p}{m}} \tag{7}$$

The ballistic limit calculated from the above proposed equation is plotted against projectile strike velocity in Fig. 9(a). To match the experimental values, the points indicating the perforation of RC slabs must lie below the line of equality. The points indicating no-perforation, however, should lie above the equality line. The figure shows that the equality line clearly separates the perforation data from non-perforation data with the exception of one data point, which too is very close to the equality line. It is due to this reason that no error band is shown in this figure. This clearly illustrates that the proposed equation shows a strong correlation between the dynamic perforation energy and the energy required for quasi-static perforation for slabs cast with different rebar spacing varying from very small spacing, essentially requiring rupture of rebars for perforation, to the large spacing necessitating the only perforation of concrete without any interaction with rebars. A comparison of the predicted ballistic limit using UKAEA formula with the experimental values is also plotted in Fig. 9(b), which shows poor performance of the model because the equality line is not separating the perforation data from the non-perforation data even after the consideration of 15% error band.

It is worth mentioning that the behavior of RC under the impact of projectiles (at varying strike velocities), especially in the estimation of ballistic limit, is governed by

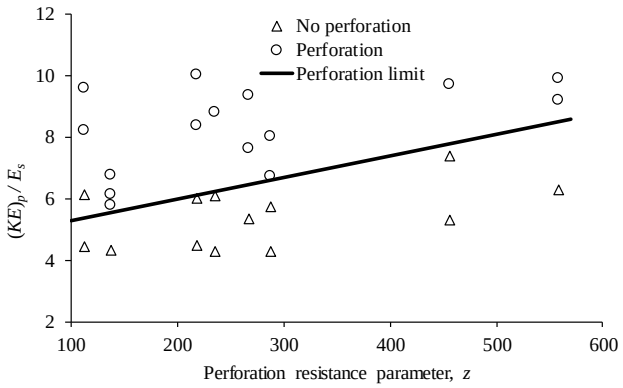

Fig. 8 Variation of $(KE)_p$ / E_s with perforation resistance parameter, z. ($(KE)_p$ = projectile kinetic energy at strike, E_s = energy absorbed in quasi-static punching)

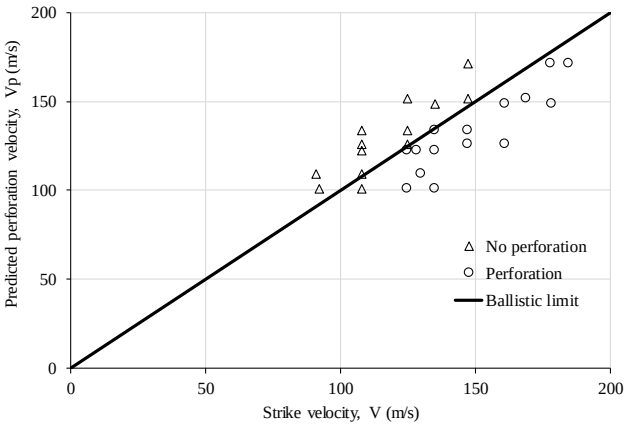

Fig. 9 Prediction of ballistic limit (a) based on energy absorbed in quasi-static punching (b) based on UKAEA formula (Li *et al.* 2005)

the complete stress-strain pattern of rebars. This is because the state of stress in different rebars varies from elastic state to fracture. Moreover, the value of E_s estimated from the quasi-static response is also dependent on the complete stress-strain pattern of rebars as the post-peak response is also involved in the calculation of E_s. Thus, it was not feasible to account for the difference in the material properties of the two types of rebars for achieving the equivalent reinforcement ratio.

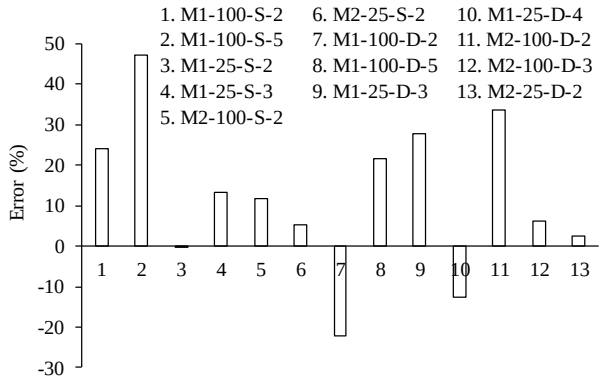

Fig. 10 Error in the prediction of penetration depths

5.2 Prediction of penetration depth

In the present study, penetration depth was predicted employing the following modified NDRC equations (NDRC 1945):

$$\left.\begin{aligned} \frac{x}{d} &= 2G^{0.5} \text{ for } G \le 1 \\ \frac{x}{d} &= G + 1 \text{ for } G \ge 1 \end{aligned}\right\} \quad (8)$$

$$\text{Here, } G = \text{Impact function} = \frac{3.8\times10^{-5} N M V_1^{1.8}}{\sqrt{f_c'}\, d^{2.8}} \quad (9)$$

(SI units)

In the above equation, V_1=projectile impact velocity (m/s); N=projectile nose shape factor; M=mass of the projectile (kg); f_c' =compressive strength of concrete (N/m^2); x=penetration depth (m); and d=projectile aft body diameter (m).

Fig. 10 illustrates error in the prediction of the penetration depth for all those tested slabs which did not experience full perforation. The prediction appears to be reasonable as the majority of the data is lying within an error range of 0 to 20%. The prediction shows underestimation or overestimation based on the sign of the error. The positive sign of the error indicates an overestimation, whereas negative sign shows the underestimation. This confirms the applicability of the modified NDRC equation for the prediction of penetration depth in RC slabs having different rebar patterns and spacing.

5. Conclusions

The following conclusions can be drawn from the present experimental and analytical study:

- The steel bar configuration in concrete slabs plays a significant role in controlling the damage under hard projectile impact. The reduction in the spacing of rebars on the back face of slab (without altering the overall percentage of reinforcing steel) is substantially more influential in reducing the impact damage than the placement of extra rebars on the impact face (i.e. doubly reinforced).
- The damage in quasi-static punching due to spherical nose penetrator in doubly reinforced slabs is substantially smaller than the singly reinforced slabs. The quasi-static penetration of RC slabs develops two peaks in load-displacement curves with the 2nd peak being lower than the 1st peak. The decrease in rebar spacing causes substantial enhancement in the 2nd peak load, which leads to an increase in the perforation energy. The increase in concrete grade also leads to the development of second peak even for wider rebar spacing.
- The front and back crater sizes caused by projectile impact are generally smaller in doubly reinforced slabs than singly reinforced slabs. Despite having larger crater diameter, the ejected weight in 25 mm spaced rebar slabs is less in comparison to 100 mm spaced rebar slabs. The change in the ejected weight gets enhanced with the increase in the concrete strength.
- For the doubly reinforced slabs, the front face crater diameter, and the ejected weight are lesser than the singly reinforced slabs. However, they are more than the singly reinforced slabs for the rear face.
- The energy absorbed in quasi-static punching of concrete slabs is used to predict equations for the ballistic limit. The proposed equations show a strong correlation between the dynamic perforation energy and the energy required for quasi-static perforation of slabs.
- The penetration depth in RC slabs having different rebar spacing was also predicted using modified NDRC equation illustrating prediction with acceptable error.

Acknowledgement

The authors are grateful to the Deanship of Scientific Research, King Saud University, for funding through Vice Deanship of Scientific Research Chairs.

References

Abbas, H., Abadel, A.A., Almusallam, T. and Al-Salloum, Y. (2015), "Effect of CFRP and TRM strengthening of RC slabs on punching shear strength", *Latin American J. Solids Struct.*, **12**(9), 1616–1640. https://doi.org/10.1590/1679-78251277.

Abbas, H., Paul, D.K., Godbole, P.N. and Nayak, G.C. (1996), "Aircraft crash upon outer containment of nuclear power plant", *Nuclear Eng. Design*, **160**(1–2), 13–50. https://doi.org/10.1016/0029-5493(95)01049-1.

Abdel-Kader, M. and Fouda, A. (2014), "Effect of reinforcement on the response of concrete panels to impact of hard projectiles", *J. Impact Eng.*, **63**, 1–17. https://doi.org/10.1016/j.ijimpeng.2013.07.005.

ACI Committee 318. (2014), Building Code Requirements for Structural Concrete (ACI 318-14) and Commentary on Building Code Requirements for Structural Concrete (ACI 318R-14), American Concrete Institute, MI, USA.

Al-Gasham, T.S., Mhalhal, J.M. and Jabir, H.A. (2019), "Improving punching behavior of interior voided slab-column connections using steel sheets", *Eng. Struct.*, **199**, 109614. https://doi.org/10.1016/j.engstruct.2019.109614.

Almusallam, T.H., Abadel, A.A., Al-Salloum, Y.A., Siddiqui, N.A. and Abbas, H. (2015), "Effectiveness of hybrid-fibers in

improving the impact resistance of RC slabs", *J. Impact Eng.*, **81**, 61–73. https://doi.org/10.1016/j.ijimpeng.2015.03.010.

Almusallam, T.H., Siddiqui, N.A., Iqbal, R.A. and Abbas, H. (2013), "Response of hybrid-fiber reinforced concrete slabs to hard projectile impact", *J. Impact Eng.*, **58**, 17–30. https://doi.org/10.1016/j.ijimpeng.2013.02.005.

ASTM. (2014), "A370: Standard Test Methods and Definitions for Mechanical Testing of Steel Products", ASTM International, PA, USA.

ASTM. (2020), "C39-20 Standart test method for compressive strength of cylindrical concrete specimens", ASTM International, PA, USA.

Dancygier, A.N. (1997), "Effect of reinforcement ratio on the resistance of reinforced concrete to hard projectile impact", *Nuclear Eng. Design*, **172**(1–2), 233–245. https://doi.org/10.1016/s0029-5493(97)00055-1.

Dancygier, A.N., Yankelevsky, D.Z. and Jaegermann, C. (2007), "Response of high performance concrete plates to impact of non-deforming projectiles", *J. Impact Eng.*, **34**(11), 1768–1779. https://doi.org/10.1016/j.ijimpeng.2006.09.094.

Dönmez, A. and Bažant, Z.P. (2017), "Size effect on punching strength of reinforced concrete slabs with and without shear reinforcement", *ACI Struct. J.*, **114**(4), 875-886. http://www.cee.northwestern.edu/people/bazant/PDFs/Papers/581.pdf

Fullard, K., Baum, M.R. and Barr, P. (1991), "The assessment of impact on nuclear power plant structures in the United Kingdom", *Nuclear Eng. Design*, **130**(2), 113-120. https://doi.org/10.1016/0029-5493(91)90120-7.

Goswami, A., Adhikary, S.D. and Li, B. (2019), "Predicting the punching shear failure of concrete slabs under low velocity impact loading", *Eng. Struct.*, **184**, 37-51. https://doi.org/10.1016/j.engstruct.2019.01.081.

Li, J., Wu, C., Hao, H. and Su, Y. (2017), "Experimental and numerical study on steel wire mesh reinforced concrete slab under contact explosion", *Mater. Design*, **116**, 77–91. https://doi.org/10.1016/j.matdes.2016.11.098.

Li, Q.M., Reid, S.R., Wen, H.M. and Telford, A.R. (2005), "Local impact effects of hard missiles on concrete targets", *J. Impact Eng.*, **32**(1-4), 224-284. https://doi.org/10.1016/j.ijimpeng.2005.04.005.

Mazek, S. A. and Wahab, M. M. A. (2015), "Impact of composite materials on buried structures performance against blast wave", *Struct. Eng. Mech.*, **53**(3), 589–605. https://doi.org/10.12989/sem.2015.53.3.589.

Murali, G. and Ramprasad, K. (2018), "A feasibility of enhancing the impact strength of novel layered two stage fibrous concrete slabs", *Eng. Struct.*, **175**, 41–49. https://doi.org/10.1016/j.engstruct.2018.08.034.

NDRC. (1945), *Effects of Impact and Explosion. Summary Technical Report of Division 2, Vol 1*, National Defense Research Committee, Washington, DC., USA.

Oh, H. and Sim, J. (2004), "Punching shear strength of strengthened deck panels with externally bonded plates", *Compos. Part B Eng.*, **35**(4), 313–321. https://doi.org/10.1016/j.compositesb.2003.12.003.

Öncü, M. E., Yön, B., Akkoyun, Ö. and Taşkiran, T. (2015), "Investigation of blast-induced ground vibration effects on rural buildings", *Struct. Eng. Mech.*, **54**(3), 545–560. https://doi.org/10.12989/sem.2015.54.3.545.

Peng, Y., Wu, H., Fang, Q., Liu, J.Z. and Gong, Z.M. (2016), "Residual velocities of projectiles after normally perforating the thin ultra-high performance steel fiber reinforced concrete slabs", *J. Impact Eng.*, **97**, 1–9. https://doi.org/10.1016/j.ijimpeng.2016.06.006.

Rajput, A. and Iqbal, M.A. (2017), "Impact behavior of plain, reinforced and prestressed concrete targets", *Mater. Design*, **114**, 459–474. https://doi.org/10.1016/j.matdes.2016.10.073.

Reinhardt, H.W. and Walraven, J.C. (1982), "Cracks in Concrete Subject to Shear", *ASCE J Struct Div*, **108**(ST1), 207–224. https://cedb.asce.org/CEDBsearch/record.jsp?dockey=0033755.

Rochdi, E.H., Bigaud, D., Ferrier, E. and Hamelin, P. (2006), "Ultimate behavior of CFRP strengthened RC flat slabs under a centrally applied load", *Compos. Struct.*, **72**(1), 69–78. https://doi.org/10.1016/j.compstruct.2004.10.017.

Siddiqui, N.A. and Abbas, H. (2002), "Mechanics of missile penetration into geo-materials", *Struct. Eng. Mech.*, **13**(6), 639–652. https://doi.org/10.12989/sem.2002.13.6.639.

Siddiqui, N.A., Khateeb, B.M.A., Almusallam, T.H., Al-Salloum, Y.A., Iqbal, R.A. and Abbas, H. (2014a), "Reliability of RC shielded steel plates against the impact of sharp nose projectiles", *J. Impact Eng.*, **69**, 122–135. https://doi.org/10.1016/j.ijimpeng.2014.03.001.

Siddiqui, N.A., Khateeb, B.M.A., Almusallam, T.H. and Abbas, H. (2014b), "Reliability of double-wall containment against the impact of hard projectiles", *Nuclear Eng. Design*, **270**, 143–151. https://doi.org/10.1016/j.nucengdes.2014.01.003.

Siddiqui, N.A., Kumar, S., Khan, M.A. and Abbas, H. (2006), "A simplified procedure to incorporate soil non-linearity in missile penetration problems", *Struct. Eng. Mech.*, **23**(3), 249–262. https://doi.org/10.12989/sem.2006.23.3.249.

Sohn, J.M., Kim, S. J., Seong, D.J., Kim, B.J., Ha, Y.C., Seo, J. K. and Paik, J.K. (2014), "Structural impact response characteristics of an explosion-resistant profiled blast walls in arctic conditions", *Struct. Eng. Mech.*, **51**(5), 755–771. https://doi.org/10.12989/sem.2014.51.5.755.

Tamayo, J.L.P. and Awruch, A.M. (2016), "Numerical simulation of reinforced concrete nuclear containment under extreme loads", *Struct. Eng. Mech.*, **58**(5), 799-823. https://doi.org/10.12989/sem.2016.58.5.799.

Thai, D.K. and Kim, S.E. (2015), "Numerical simulation of reinforced concrete slabs under missile impact", *Struct. Eng. Mech.*, **53**(3), 455-479. https://doi.org/10.12989/sem.2015.53.3.455.

Verma, M., Prem, P.R., Rajasankar, J. and Bharatkumar, B.H. (2016), "On low-energy impact response of ultra-high performance concrete (UHPC) panels", *Mater. Design*, **92**, 853-865. https://doi.org/10.1016/j.matdes.2015.12.065.

Wang, J., Yuan, W., Wu, X. and Wei, K. (2017), "Dynamic performance of girder bridges with explosion-proof and aseismic system", *Struct. Eng. Mech.*, **61**(3), 419-426. https://doi.org/10.12989/sem.2017.61.3.419.

Wu, H., Fang, Q., Peng, Y., Gong, Z. M. and Kong, X. Z. (2015), "Hard projectile perforation on the monolithic and segmented RC panels with a rear steel liner", *J. Impact Eng.*, **76**, 232–250. https://doi.org/10.1016/j.ijimpeng.2014.10.010.

Xu, X., Ma, T. and Ning, J. (2019), "Failure mechanism of reinforced concrete subjected to projectile impact loading", *Eng. Failure Analysis*, **96**, 468-483. https://doi.org/10.1016/j.engfailanal.2018.11.006.

Zineddin, M. and Krauthammer, T. (2007), "Dynamic response and behavior of reinforced concrete slabs under impact loading", *J. Impact Eng.*, **34**(9), 1517–1534. https://doi.org/10.1016/j.ijimpeng.2006.10.012.

CC